

UNCERTAINTY-AWARE PROTOTYPE LEARNING WITH VARIATIONAL INFERENCE FOR FEW-SHOT POINT CLOUD SEGMENTATION

Yifei Zhao¹ Fanyu Zhao² Yinsheng Li³

Fudan University, Shanghai, China
 {yfzhao19, fyzhao20, liys}@fudan.edu.cn

ABSTRACT

Few-shot 3D semantic segmentation aims to generate accurate semantic masks for query point clouds with only a few annotated support examples. Existing prototype-based methods typically construct compact and deterministic prototypes from the support set to guide query segmentation. However, such rigid representations are unable to capture the intrinsic uncertainty introduced by scarce supervision, which often results in degraded robustness and limited generalization. In this work, we propose **UPL** (Uncertainty-aware Prototype Learning), a probabilistic approach designed to incorporate uncertainty modeling into prototype learning for few-shot 3D segmentation. Our framework introduces two key components. First, UPL introduces a dual-stream prototype refinement module that enriches prototype representations by jointly leveraging limited information from both support and query samples. Second, we formulate prototype learning as a variational inference problem, regarding class prototypes as latent variables. This probabilistic formulation enables explicit uncertainty modeling, providing robust and interpretable mask predictions. Extensive experiments on the widely used ScanNet and S3DIS benchmarks show that our UPL achieves consistent state-of-the-art performance under different settings while providing reliable uncertainty estimation. The code is available at [fduelab-upl.github.io](https://github.com/fduelab-upl).

Index Terms— few-shot learning; point cloud segmentation; prototype learning; variational inference; uncertainty estimation

1. INTRODUCTION

3D point cloud segmentation aims to assign a semantic label to each point and has broad applications in autonomous driving [1, 2], robotics [3, 4], and AR/VR [5, 6]. Recent advances, such as Mask3D [7] and OneFormer3D [8], have achieved remarkable results when trained on large-scale annotated datasets. However, constructing such datasets with dense point-level annotations is both costly and time-consuming [9, 10]. To alleviate this issue, few-shot point cloud semantic segmentation (FS-PCS) has been introduced, aiming to generalize segmentation models to novel classes with only a limited number of labeled samples [11, 12].

Generally, FS-PCS follows an episodic meta-learning paradigm, where each episode consists of a support set with a few annotated scenes and a query set. Most existing FS-PCS methods adopt a prototype-based approach, in which prototypes derived from the support scenes are subsequently used to guide the segmentation of the query scenes [13, 14, 15]. Building on this paradigm, recent works incorporate advanced techniques, such as graph convolutions [16] and attention mechanisms [17], to improve segmentation

performance. Despite their success, these methods construct deterministic prototypes to perform segmentation, neglecting the inherent uncertainty in few-shot scenarios with scarce supervision. To this end, such deterministic prototypes lead to two key drawbacks: (1) deterministic prototypes often fail to produce reliable segmentation when facing large intra-class variability and strong inter-class similarity [18]. Addressing this challenge requires the model to generate more robust and discriminative prototypes that can generalize effectively under limited supervision. (2) deterministic prototypes are incapable of modeling the uncertainty of predictions. Uncertainty estimation improves model interpretability and reliability, especially with few samples. While probabilistic modeling has been preliminarily explored for few-shot 2D segmentation [19] and uncertainty estimation studied in point cloud segmentation [20], FS-PCS methods have largely neglected uncertainty modeling.

To address these challenges, we propose UPL, a probabilistic framework for few-shot 3D segmentation that enables uncertainty-aware prototype learning. Specifically, UPL introduces two main components: (i) a dual-stream prototype refinement (DPR) module, which integrates both support and query information through channel-wise attention. To this end, this module produces richer and more discriminative prototypes, which help mitigate intra-class variability and inter-class similarity. (ii) a variational prototype inference regularization (VPIR) module. It formulates prototype learning as a variational inference problem, where class prototypes are treated as latent variables. During model training, the Kullback-Leibler divergence aligns the prior prototype distribution derived from support data with the posterior prototype distribution derived from query data. During inference, by sampling multiple Monte Carlo samples from prior prototype distribution, our UPL yields not only robust mask predictions but also reliable uncertainty estimation.

To the best of our knowledge, this is the first work that models uncertainty in few-shot point cloud segmentation. We conduct extensive experiments on two widely used benchmarks, S3DIS[21] and ScanNet[22], under different few-shot settings. The results demonstrate that UPL consistently achieves state-of-the-art performance while providing robust and interpretable uncertainty estimation. Our main contributions are summarized as follows:

- We propose UPL, a probabilistic framework for FS-PCS that formulates few-shot learning as variational inference, modeling class prototypes as latent variables to enable uncertainty-aware 3D segmentation.
- We introduce a dual-stream prototype refinement module, which effectively integrates information from both support and query sets, producing more discriminative prototypes.
- Extensive experiments on S3DIS and ScanNet show that UPL achieves consistent state-of-the-art performance and provides reliable uncertainty estimation for FS-PCS tasks.

¹ and ² contributed equally to this work; ³ is the corresponding author.

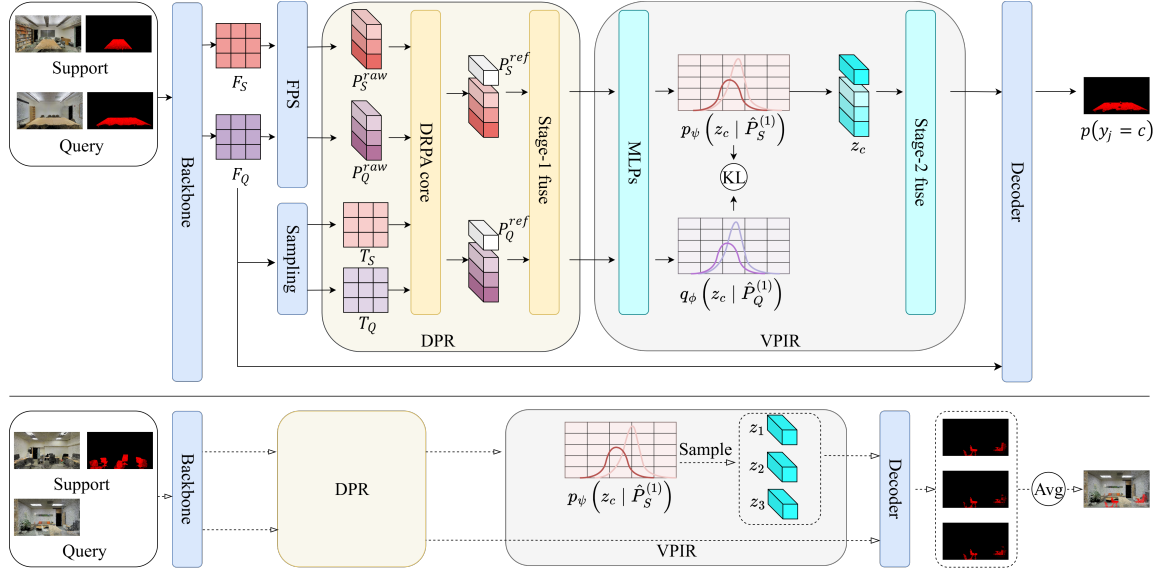


Fig. 1. Overview of our UPL framework. UPL consists of two primary modules: (i) the Dual-stream Prototype Refinement (DPR) module, which enhances prototype discriminability by leveraging mutual information between support and query sets, and (ii) the Variational Prototype Inference Regularization (VPIR) module, which models class prototypes as latent variables to capture uncertainty and enable probabilistic inference. The solid lines indicate the training process, while the dashed lines represent the inference process.

2. PRELIMINARIES

We follow the episodic N -way K -shot setting, with disjoint base C_{base} and novel C_{novel} classes [23, 24]. Each episode includes a support set $\{(\mathbf{P}t_i^s, \mathbf{Y}_i^s)\}_{i=1}^{NK}$ and a query set $\{(\mathbf{P}t^q, \mathbf{Y}^q)\}$. Each point cloud $\mathbf{P}t \in \mathbb{R}^{n \times d_{pt}}$ is encoded via a backbone f_θ into per-point features:

$$\mathbf{F} = f_\theta(\mathbf{P}t) \in \mathbb{R}^{n \times d_f}. \quad (1)$$

Class prototypes are constructed by applying Farthest Point Sampling (FPS) [13] to the feature set \mathbf{F} . For each class c , FPS selects a set of representative points, and their features are averaged to obtain sub-prototypes:

$$\mathbf{p}_c^{raw} = \frac{1}{|\mathbf{P}t_c|} \sum_{i \in \mathbf{P}t_c} \mathbf{F}_i, \quad (2)$$

where $\mathbf{P}t_c$ denotes the set of points assigned to class c by FPS. The set of all class prototypes is denoted as $\mathbf{P}^{raw} = [\mathbf{p}_1^{raw}, \dots, \mathbf{p}_C^{raw}] \in \mathbb{R}^{C \times d_p}$. If the number of available points is less than the desired sample size, zero-padding is used.

Notation: \mathbf{P}_*^{raw} and \mathbf{P}_*^{ref} denote the collections of raw, refined prototypes for all classes in the support set, where $*$ denotes either S or Q . \mathbf{Z} denotes variational prototypes.

3. METHODOLOGY

3.1. Overview

As illustrated in Fig. 1, the proposed framework consists of two key components: (i) a Dual-stream Prototype Refinement (DPR) module, which refines raw prototypes derived from both support and query sets using shared token attention to enhance their discriminative power; and (ii) a Variational Prototype Inference Regularization (VPIR) module, which models class prototypes as latent variables to capture uncertainty and enable probabilistic inference. Specifically, the DPR module generates refined prototypes by leveraging mutual information between support and query features, reducing intra-class variability and inter-class confusion. The

VPIR module formulates prototype learning as a variational inference problem, where class prototypes are treated as Gaussian latent variables. During training, the posterior distribution aligns with the prior via KL divergence, while during inference, multiple samples from the prior distribution are used to generate robust predictions. Finally, the framework integrates raw, refined, and variational prototypes through a two-stage fusion process to produce the final representation, enabling accurate and uncertainty-aware predictions.

3.2. Dual-stream Prototype Refinement

We introduce the *Dual-stream Prototype Refinement* (DPR) module to refine support and query prototypes via mutual interaction. Let $\mathbf{T}_S, \mathbf{T}_Q \in \mathbb{R}^{B \times d \times N}$ denote the support and query token sets, and $\mathbf{P}_S^{raw}, \mathbf{P}_Q^{raw}$ be the corresponding raw class prototypes, obtained via masked average pooling over labeled points. DPR performs two symmetric value-substitution passes using shared attention to refine both streams concurrently:

$$\mathbf{P}_S^{ref}, \mathbf{P}_Q^{ref} = \text{DPR}(\mathbf{T}_Q, \mathbf{T}_S, \mathbf{P}_S^{raw}, \mathbf{P}_Q^{raw}), \quad (3)$$

where attention weights are computed in a channel-wise manner via scaled dot-product between tokens.

These weights modulate the prototype update through a value-substitution operation, followed by a 1D convolution and residual connection:

$$\mathbf{P}_*^{ref} = \text{LN}(\mathbf{P}_*^{raw} + \text{Conv1d}(\mathbf{A} \cdot \text{Linear}(\mathbf{P}_*^{raw}))), \quad (4)$$

where $*$ $\in \{S, Q\}$. Layer normalization and learned projections enhance optimization stability and feature expressiveness.

To aggregate refined features with raw ones, we apply an adaptive fusion gate:

$$\hat{\mathbf{p}}_c^{(1)} = (1 - \alpha_c)\mathbf{p}_c^{raw} + \alpha_c\mathbf{p}_c^{ref}, \quad \alpha_c = \sigma([\mathbf{p}_c^{raw} \parallel \mathbf{p}_c^{ref}]), \quad (5)$$

where $\sigma(\cdot)$ denotes the sigmoid activation. This allows the model to control class-wise refinement adaptively.

Table 1. Few-shot 3D semantic segmentation mIoU (%) on S3DIS[21] and ScanNet[22] under N -way K -shot settings, following the standardized CoSeg benchmark [15]. S0 / S1: two split seeds; Mean: average. Best in bold.

	Methods	1-way 1-shot			1-way 5-shot			2-way 1-shot			2-way 5-shot		
		S0	S1	Mean									
S3DIS[21]	AttMPTI[13]	36.32	38.36	37.34	46.71	42.70	44.71	31.09	29.62	30.36	39.53	32.62	36.08
	QGE[25]	41.69	39.09	40.39	50.59	46.41	48.50	33.45	30.95	32.20	40.53	36.13	38.33
	QPGA[18]	35.50	35.83	35.67	38.07	39.70	38.89	25.52	26.26	25.89	30.22	32.41	31.32
	CoSeg[15]	46.31	48.10	47.21	51.40	48.68	50.04	37.44	36.45	36.95	42.27	38.45	40.36
	UPL (ours)	48.18	49.02	48.60	55.92	48.53	52.22	38.13	37.44	37.79	41.78	41.96	41.87
ScanNet[22]	AttMPTI[13]	34.03	30.97	32.50	39.09	37.15	38.12	25.99	23.88	24.94	30.41	27.35	28.88
	QGE[25]	37.38	33.02	35.20	45.08	41.89	43.49	26.85	25.17	26.01	28.35	31.49	29.92
	QPGA[18]	34.57	33.37	33.97	41.22	38.65	39.94	21.86	21.47	21.67	30.67	27.69	29.18
	CoSeg[15]	41.73	41.82	41.78	48.31	44.11	46.21	28.72	28.83	28.78	35.97	33.39	34.68
	UPL (ours)	43.13	42.87	43.00	48.48	45.18	46.83	32.09	32.68	32.39	39.65	37.15	38.40

3.3. Variational Prototype Inference Regularization

To model uncertainty and intra-class variation, we treat each class prototype as a latent variable drawn from a Gaussian distribution. Specifically, we define a prior $p_\psi(z_c)$ based on fused support features $\hat{\mathbf{p}}_c^{(1)}$, and a posterior $q_\phi(z_c)$ based on query features \mathbf{p}_c^q . Both distributions are parameterized by MLPs that produce the corresponding mean and variance.

During training, we use the reparameterization trick to sample prototypes from the prior, i.e., $z_c = \mu_c^{pr} + \sigma_c^{pr} \odot \epsilon$, where $\epsilon \sim \mathcal{N}(\mathbf{0}, \mathbf{I})$. A KL divergence is computed between the posterior and prior:

$$\mathcal{L}_{\text{KL}} = \sum_c \text{KL}(q_\phi(z_c) \parallel p_\psi(z_c)), \quad (6)$$

which regularizes the distribution during optimization.

To integrate the sampled prototype into the final representation, we apply a learnable fusion gate between the deterministic prototype $\hat{\mathbf{p}}_c^{(1)}$ and the sampled z_c :

$$\hat{\mathbf{p}}_c^{(2)} = (1 - \beta_c)\hat{\mathbf{p}}_c^{(1)} + \beta_c z_c, \quad (7)$$

where β_c is obtained via a sigmoid gate over the concatenated inputs.

At test time, multiple samples $\{z_c^{(t)}\}_{t=1}^T$ are drawn from the prior to form an ensemble prediction, and we average the logits over T stochastic forward passes.

3.4. Uncertainty Estimation and Learning Objective

To quantify predictive uncertainty, we adopt a Monte Carlo ensemble approach using T prior samples during inference. The predicted class probability for query point j is computed as the average over T softmax-normalized outputs:

$$p_{j,c} = \frac{1}{T} \sum_{t=1}^T \text{softmax}(\ell_{j,c}^{(t)}), \quad (8)$$

where $\ell_{j,c}^{(t)}$ denotes the similarity-based logit obtained using the t -th sampled prototype.

Uncertainty is estimated via two complementary measures. First, we compute prediction variance across samples, which captures epistemic uncertainty. Second, we optionally compute the entropy of the mean prediction distribution, reflecting overall confidence. Both metrics are fused to yield per-point uncertainty maps.

The overall training objective combines three components:

$$\mathcal{L} = \mathcal{L}_{\text{seg}} + \mathcal{L}_{\text{base}} + \beta(e)\mathcal{L}_{\text{KL}}, \quad (9)$$

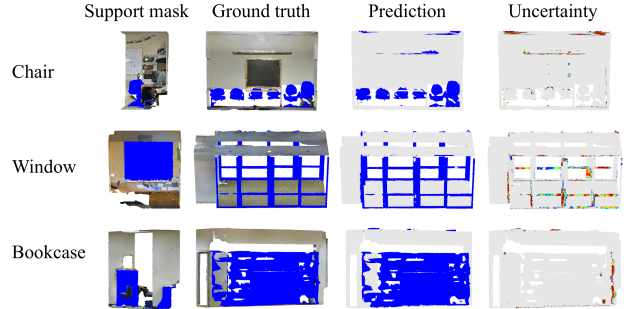


Fig. 2. Qualitative results of UPL on S3DIS. UPL yields not only accurate mask prediction but also reliable uncertainty estimation.

where \mathcal{L}_{seg} is the supervised segmentation loss on novel-class queries, $\mathcal{L}_{\text{base}}$ is the auxiliary base-class supervision loss (following [15]), and \mathcal{L}_{KL} is the KL divergence defined in Eq. 6. The weight $\beta(e)$ follows a linear warm-up schedule with training epoch e .

4. EXPERIMENTS

4.1. Experimental Setup

Datasets. Following CoSeg [15], we evaluate our model on two widely used FS-PCS benchmarks, i.e. S3DIS[21] and ScanNet[22]. Both datasets are split into disjoint base and novel classes, and we adopt the episodic N -way K -shot setting. In each episode, K support fragments and one query scene are sampled for N novel classes. **Evaluation Metrics.** Following prior work [15], we apply denser support sampling and improved class balancing to mitigate foreground leakage issues observed in earlier setups. We report mean Intersection over Union (mIoU, %) over novel classes, averaged across two random seeds (S0/S1) and four few-shot settings: 1-way 1-shot, 1-way 5-shot, 2-way 1-shot, and 2-way 5-shot.

4.2. Main Results

Table 1 reports mIoU on S3DIS and ScanNet under the four standard few-shot settings (averaged over S0/S1). UPL consistently outperforms all baselines on both datasets. On S3DIS, UPL attains 48.60, 52.22, 37.79, and 41.87 mIoU, surpassing the strongest baseline (CoSeg) by up to +2.18 points. On ScanNet, it obtains 43.00, 46.83, 32.39, and 38.40 mIoU, with even larger gains in the 2-way settings (+3.61 and +3.72). These improvements are consistent across seeds and align with our design: (i) the dual-stream prototype refinement leverages query features to reduce intra-class variability and

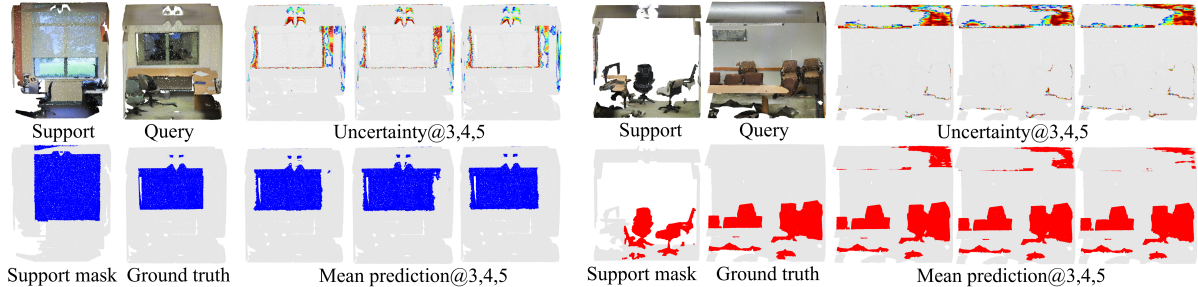


Fig. 3. Visualization of uncertainty analysis for the 1-way 1-shot setting. The left panel highlights the foreground class **window** (in blue), while the right panel focuses on the class **chair** (in red). Uncertainty is represented using a heatmap, where values transition from blue (low uncertainty) to red (high uncertainty). The number following @ denotes the sampling times T .

Table 2. Ablation study of DPR and VPIR modules on ScanNet (2-way). Performance is reported as mIoU (%).

DPR	VPIR	2-way 1-shot	2-way 5-shot
		27.32	33.65
	✓	30.19	36.04
✓	✓	32.39	38.40

inter-class confusion, and the variational prototype inference regularization module that enables uncertainty-aware prototype learning. Fig. 2 provides qualitative results on S3DIS. As shown in the figure, UPL produces cleaner object boundaries and suppresses spurious activations in ambiguous regions (e.g., class boundaries and cluttered areas). More importantly, UPL also outputs uncertainty maps alongside the segmentation masks, which clearly highlight regions of occlusion and label ambiguity. This not only improves the interpretability of the predictions but also demonstrates the reliability of our uncertainty-aware prototype learning framework.

Effect of K . As expected, increasing the number of support examples (K) consistently improves performance for all methods. Notably, UPL benefits more from larger K . For example, on S3DIS the gain from 1w1s to 1w5s is +3.62 points, compared to only +2.83 for the strongest baseline. This indicates that UPL adapts more effectively to intra-class variation, thanks to stochastic prototype sampling in the variational inference module.

Effect of N . Increasing the number of novel classes (N) makes the task more challenging by introducing greater inter-class ambiguity. Although performance decreases for all methods, UPL preserves a larger fraction of its 1-way accuracy than competing approaches. This demonstrates the effectiveness of dual-stream refinement and variational inference in mitigating class overlap and maintaining robust segmentation under more complex settings.

4.3. Ablation Study

Benefits of DPR. Table 2 reports the ablation study of the dual-stream refinement prototype attention (DPR) and variational prototype inference regularization (VPIR) modules on ScanNet under both 2-way 1-shot and 5-shot settings. Both modules individually improve performance compared to the baseline without them. Specifically, DPR alone brings notable gains (+5.07 and +4.75 mIoU in 1-shot and 5-shot, respectively), demonstrating the importance of jointly leveraging support and query features to construct more discriminative prototypes.

Benefits of VPIR. VPIR alone also provides clear improvements (+2.87 and +2.39), validating the effectiveness of modeling prototypes as distributions for robust estimation. When combined, DPR and VPIR achieve the best results (32.39 and 38.40), showing complementary benefits: refinement reduces intra/inter-class confusion,

Table 3. Effect of the number of prior samples T on S3DIS under 1-way settings. Performance is reported as mIoU (%).

T	1-way 1-shot	1-way 5-shot
3	48.60	52.22
4	50.32	53.18
5	51.69	53.06

while variational inference further enhances robustness through uncertainty-aware prototype learning.

Impact of Prior Sampling. Table 3 shows the effect of varying the number of prior samples T during inference on the S3DIS dataset under 1-way settings. As T increases from 3 to 5, mIoU improves from 48.60% (**Expected Calibration Error** 0.1710) to 51.69% (0.0567) in the 1-shot case, while in the 5-shot case, the best performance (53.18%) occurs at $T = 4$. These results demonstrate that leveraging multiple stochastic samples enhances prediction stability, though the optimal number of samples may vary with supervision strength. The improvement reflects the ensemble-like benefits of Monte Carlo sampling, which mitigates prediction variance and leads to more reliable few-shot performance.

Analysis of Uncertainty. Fig. 3 visualizes the uncertainty maps produced by our framework. High uncertainty is primarily concentrated along object boundaries and in ambiguous regions, such as the **chair** and **window** classes. Importantly, incorrect predictions tend to correlate with higher uncertainty, which is clearly reflected by the shift from blue (low) to red (high) in the heatmaps. These observations highlight two key advantages of our probabilistic design: (i) it provides interpretable uncertainty estimates that can guide the identification of error-prone regions, and (ii) it improves prediction reliability, as increasing T reduces uncertainty and corrects misclassifications. Together, these results demonstrate that our method contributes both to performance gains and to model interpretability.

5. CONCLUSION

In this work, we introduced **UPL**, a probabilistic framework for few-shot 3D point cloud segmentation that enables uncertainty-aware prototype learning. UPL incorporates a dual-stream prototype refinement module to construct more discriminative prototypes, and a variational prototype inference regularization module to treat prototypes as latent variables, allowing explicit uncertainty modeling. Through extensive experiments on the S3DIS and ScanNet benchmarks, UPL achieves state-of-the-art performance while providing robust and interpretable uncertainty estimation. Our study highlights the importance of modeling uncertainty in few-shot point cloud segmentation. We believe this work opens up promising directions for extending uncertainty-aware learning to broader 3D tasks.

6. ACKNOWLEDGMENTS

This research was supported by the National Key Research and Development Program of China (No.2023YFC3304800). The computations in this research were performed using the CFFF platform of Fudan University. Deployed on the Cross-Border Trade Payment Intelligent Agent Platform (<https://fdueblab.cn/>).

7. REFERENCES

- [1] Hafsa Benallal, Nadine Abdallah Saab, Hamid Tairi, Ayman Alfalou, and Jamal Riffi, “Advancements in semantic segmentation of 3d point clouds for scene understanding using deep learning,” *Technologies*, vol. 13, no. 8, 2025.
- [2] Yuxuan Bi, Peng Liu, Tianyi Zhang, Jialin Shi, and Caixia Wang, “Multi-scale sparse convolution and point convolution adaptive fusion point cloud semantic segmentation method,” *Scientific Reports*, vol. 15, no. 1, pp. 4372, 2025.
- [3] Haoming Lu and Humphrey Shi, “Deep learning for 3d point cloud understanding: A survey,” *CoRR*, vol. abs/2009.08920, 2020.
- [4] Yulan Guo, Hanyun Wang, Qingyong Hu, Hao Liu, Li Liu, and Mohammed Bennamoun, “Deep learning for 3d point clouds: A survey,” *IEEE Trans. Pattern Anal. Mach. Intell.*, vol. 43, no. 12, pp. 4338–4364, 2021.
- [5] Roberto Pierdicca, Marina Paolanti, Francesca Matrone, Massimo Martini, Christian Morbidoni, Eva Savina Malinverni, Emanuele Frontoni, and Andrea Maria Lingua, “Point cloud semantic segmentation using a deep learning framework for cultural heritage,” *Remote. Sens.*, vol. 12, no. 6, pp. 1005, 2020.
- [6] Rui Zhang, Yichao Wu, Wei Jin, and Xiaoman Meng, “Deep-learning-based point cloud semantic segmentation: A survey,” *Electronics*, vol. 12, no. 17, pp. 3642, 2023.
- [7] Jonas Schult, Francis Engelmann, Alexander Hermans, Or Litany, Siyu Tang, and Bastian Leibe, “Mask3d: Mask transformer for 3d semantic instance segmentation,” in *2023 IEEE International Conference on Robotics and Automation (ICRA)*. IEEE, 2023, pp. 8216–8223.
- [8] Maxim Kolodiazhyi, Anna Vorontsova, Anton Konushin, and Danila Rukhovich, “Oneformer3d: One transformer for unified point cloud segmentation,” in *Proceedings of the IEEE/CVF Conference on Computer Vision and Pattern Recognition*, 2024, pp. 20943–20953.
- [9] Jingyi Wang, Yu Liu, Hanlin Tan, and Maojun Zhang, “A survey on weakly supervised 3d point cloud semantic segmentation,” *IET Comput. Vis.*, vol. 18, no. 3, pp. 329–342, 2024.
- [10] Yuliang Sun, Xudong Zhang, and Yongwei Miao, “A review of point cloud segmentation for understanding 3d indoor scenes,” *Vis. Intell.*, vol. 2, no. 1, pp. 14, 2024.
- [11] Yating Xu, Conghui Hu, Na Zhao, and Gim Hee Lee, “Generalized few-shot point cloud segmentation via geometric words,” in *IEEE/CVF International Conference on Computer Vision, ICCV 2023, Paris, France, October 1-6, 2023*. 2023, pp. 21449–21458, IEEE.
- [12] Yating Xu, Na Zhao, and Gim Hee Lee, “Towards robust few-shot point cloud semantic segmentation,” in *34th British Machine Vision Conference 2023, BMVC 2023, Aberdeen, UK, November 20-24, 2023*. 2023, p. 81, BMVA Press.
- [13] Na Zhao, Tat-Seng Chua, and Gim Hee Lee, “Few-shot 3d point cloud semantic segmentation,” in *IEEE Conference on Computer Vision and Pattern Recognition, CVPR 2021, virtual, June 19-25, 2021*. 2021, pp. 8873–8882, Computer Vision Foundation / IEEE.
- [14] Canyu Zhang, Zhenyao Wu, Xinyi Wu, Ziyu Zhao, and Song Wang, “Few-shot 3d point cloud semantic segmentation via stratified class-specific attention based transformer network,” in *Proceedings of the AAAI Conference on Artificial Intelligence*, 2023, vol. 37, pp. 3410–3417.
- [15] Zhaochong An, Guolei Sun, Yun Liu, Fayao Liu, Zongwei Wu, Dan Wang, Luc Van Gool, and Serge J. Belongie, “Rethinking few-shot 3d point cloud semantic segmentation,” in *IEEE/CVF Conference on Computer Vision and Pattern Recognition, CVPR 2024, Seattle, WA, USA, June 16-22, 2024*. 2024, pp. 3996–4006, IEEE.
- [16] Bo Jiang, Ziyang Zhang, Doudou Lin, Jin Tang, and Bin Luo, “Semi-supervised learning with graph learning-convolutional networks,” in *Proceedings of the IEEE/CVF conference on computer vision and pattern recognition*, 2019, pp. 11313–11320.
- [17] Ashish Vaswani, Noam Shazeer, Niki Parmar, Jakob Uszkoreit, Llion Jones, Aidan N Gomez, Lukasz Kaiser, and Illia Polosukhin, “Attention is all you need,” *Advances in neural information processing systems*, vol. 30, 2017.
- [18] Shuting He, Xudong Jiang, Wei Jiang, and Henghui Ding, “Prototype adaption and projection for few- and zero-shot 3d point cloud semantic segmentation,” *IEEE Trans. Image Process.*, vol. 32, pp. 3199–3211, 2023.
- [19] Haochen Wang, Yandan Yang, Xianbin Cao, Xiantong Zhen, Cees Snoek, and Ling Shao, “Variational prototype inference for few-shot semantic segmentation,” in *Proceedings of the IEEE/CVF Winter Conference on Applications of Computer Vision*, 2021, pp. 525–534.
- [20] Jie Liu, Pan Zhou, Zehao Xiao, Jiayi Shen, Wenzhe Yin, Jan-Jakob Sonke, and Efstratios Gavves, “Probabilistic interactive 3d segmentation with hierarchical neural processes,” *CoRR*, vol. abs/2505.01726, 2025.
- [21] Iro Armeni, Ozan Sener, Amir R Zamir, Helen Jiang, Ioannis Brilakis, Martin Fischer, and Silvio Savarese, “3d semantic parsing of large-scale indoor spaces,” in *Proceedings of the IEEE conference on computer vision and pattern recognition*, 2016, pp. 1534–1543.
- [22] Angela Dai, Angel X Chang, Manolis Savva, Maciej Halber, Thomas Funkhouser, and Matthias Nießner, “Scannet: Richly-annotated 3d reconstructions of indoor scenes,” in *Proceedings of the IEEE conference on computer vision and pattern recognition*, 2017, pp. 5828–5839.
- [23] Oriol Vinyals, Charles Blundell, Timothy Lillicrap, Koray Kavukcuoglu, and Daan Wierstra, “Matching networks for one shot learning,” in *Proceedings of the 30th International Conference on Neural Information Processing Systems*, 2016, pp. 3637–3645.
- [24] Jake Snell, Kevin Swersky, and Richard Zemel, “Prototypical networks for few-shot learning,” *Advances in neural information processing systems*, vol. 30, 2017.
- [25] Zhenhua Ning, Zhuotao Tian, Guangming Lu, and Wenjie Pei, “Boosting few-shot 3d point cloud segmentation via query-guided enhancement,” in *Proceedings of the 31st ACM international conference on multimedia*, 2023, pp. 1895–1904.